Medicinal Chemistry & Drug Discovery

In-Silico-Inspired Design of 1,3-Diynyl Congeners of Noscapine as Promising Tubulin-Binding Anticancer Agent: Chemical Synthesis and Cellular Activity with Breast Cancer Cell Lines

Pratyush Pragyandipta,[a] Rajesh K. Meher,[a] Manas R. Naik,[b] Praveen K. R. Nagireddy,[c] Ravi K Pedapati,[c] Srinivas Kantevari,*[c] and Pradeep K. Naik*[a]

A panel of 1,3-diynyl-noscapinoids (**20**–**22**) were strategically designed to increase the anticancer activity of the lead molecule, noscapine. Structure-activity analyses revealed strong predicted free energy of binding ($\Delta G_{bind,pred}$) of −6.694, −7.294 and −7.468 kcal/mol, for **20**–**22** respectively compared to noscapine (experimental free energy of binding ($\Delta G_{bind,expt}$) is −5.246 kcal/mol). These novel derivatives were demonstrated to bind tubulin by fluorescence quenching assay and Far-UV circular dichroism. Further, they were tested to exhibit potent cytotoxic activity compared to noscapine using two human breast cancer cell lines. The IC_{50} value for noscapine, **20**, **21** and **22** has been derived to be 35.2, 27.3, 18.7 and 12.7 μM using MCF7 and 39.6, 31.4, 22.5 and 16.1 μM using MDAMB-231. These derivatives were found to arrest cell cycle in the G2/M-phase followed by apoptosis and appearance of TUNEL-positive cells. Thus, we conclude that 1,3-diynyl derivatives of noscapine have great potential to be a novel therapeutic agent for breast cancers.

Introduction

Microtubules (MTs) play a significant role in many of the cellular functions including cell division. Therefore, it has been used as a suitable drug target for the development of chemotherapeutic drugs against rapidly dividing cancer cells. The effectiveness of MT targeting drugs has been confirmed by the clinical use of vinca alkaloids and taxanes for the treatment of a wide variety of human cancers. However, these anti-MT agents are known to induce undesired, dose-limiting toxicities in patients.[1,2] The clinical success of taxanes has impelled world-wide to search for natural compounds targeted to MT but with improved characteristics. In quest for finding such a compound, without having any side effects, noscapine (an opium alkaloid) was discovered that binds tubulin dimer with a 1:1 stoichiometry, arrests a variety of mammalian cells in mitosis and causes apoptosis.[3] It has been used as a cough suppressant since the mid 1950s and illustrating a good safety profile. It is also found to be well-tolerated in humans without having any severe toxicity.[4,5,6] Furthermore, it inhibits the proliferation of cancer cells of different tissue origin and regresses effectively the implanted tumor in animal models without any side effects.[3,7–10] The minimal side effect of noscapine is due to its selectivity in killing the cancer cells without hampering the normal healthy cells. It was revealed that normal healthy cells respond to noscapine (or its tested derivatives) treatment by arresting mitosis for long period of time, at least 12 to 24 hours. However, if noscapine exposure is removed prior to this time period by replenishing with fresh drug free culture medium, the arrested cells resume the progression of the normal mitosis producing viable daughter cells.[7] This innovative research has prodded a huge enthusiasm for the scientific world to use noscapine and its synthetic analogues for the therapy of malignancy.

In order to enhance the anti-proliferative activity of noscapine we have tried to develop a new series of its derivatives (called diyne derivatives) by strategically modifying its scaffold structure and supported by our in silico efforts. These derivatives were then chemically synthesized and validated their anti-proliferative activity to cancer cells using two human carcinoma cell lines, MCF-7 and MDAMB-231. The novel derivatives were found to bind tubulin heterodimer with increased binding affinity, inhibit proliferation of neoplastic cell and causes selective G2/M arrest in cancer cells. The mitotic catastrophe in cancer cells is then followed by induction of apoptosis.

[a] *P. Pragyandipta, R. K. Meher, Prof. P. K. Naik*
Centre of Excellence in Natural Products and Therapeutics, Department of Biotechnology and Bioinformatics, Sambalpur University, Jyoti Vihar, Burla, Sambalpur-768019, Odisha, India
Phone No.: +91-9479268802
E-mail: pknaik1973@suniv.ac.in
[b] *M. R. Naik*
Department of Pharmacology, SLN Medical College Koraput-464020 Odisha, India
[c] *P. K. R. Nagireddy, R. K Pedapati, Dr. S. Kantevari*
Fluoro and Agrochemicals Division, CSIR-Indian Institute of Chemical Technology, Hyderabad 500 007, India
E-mail: ksrinivas@iict.res.in

Supporting information for this article is available on the WWW under https://doi.org/10.1002/slct.202004723

Results and Discussion

The anti-proliferative activity and tubulin binding affinity of the lead compound, noscapine, were improved many fold by orchestrating numerous intense potent derivatives.[11–15] Availability of structure activity information of these derivatives of noscapine inspired us to build up a sensible predictive model for predicting the binding affinity of newly planned derivatives and screening of potent derivatives. We are reporting in this study a panel of 1,3-diynyl derivatives of noscapine as potent tubulin binding anticancer agents.

Rational design of 1,3-diynyl derivatives of noscapine

In pursuance of our endeavours to create novel derivatives of noscapine with improved binding affinity with tubulin, we have designed a new series of derivatives by coupling of ethyne and 1,3-diyne functionality with the α-noscapine scaffold (Figure 1) based on in silico combinatorial approach. We have primarily focused on these two functional groups because both of them are recognized as a key pharmacophore in several anticancer drugs utilized in clinics such as erlotinib and icotinib (consists of ethyne group) as well as natural products such as panaxytriol, falcarinol, diplyne, 2-deoxydiplyne D sulfate, etc. (consists of 1,3-diynes group) with anticancer activity (Figure 2).[16,17]

Molecular docking and predictive binding affinity of 1,3-diynyl-noscapinoids with tubulin

The noscapinoids, reported earlier (Figure 3) and the library of 1,3-diynyl-noscapinoids (Figure 1) were docked onto the binding site of tubulin, at the interface between α- and β-tubulin using Glide XP. The predictive free energy of binding ($\triangle G_{bind,pred}$) of 1,3-diynyl derivatives of noscapine with tubulin was also calculated based on LIE-SGB predictive model. The reasonably well predictive model was developed by mapping the various energy parameters with the experimental binding affinity of training set molecules. The diverse energy terms used in the predictive model were included in Table 1. The values obtained for the coefficients α, β, γ and δ are 0.08446, −0.00223, −0.000872 and −0.45601, respectively. The $\Delta G_{bind,pred}$ of the training set molecules were found to be very close to the experimental free energy of binding ($\Delta G_{bind,expt}$) as the mean difference between both the parameters is very small (s = 0.243 kcal/mol). The quality of the fit can also be judged through the value of the squared correlation coefficient (R^2) and analysis of variance (F-value).

$$\Delta G_{bind,pred} = 0.08446 < U_{vdw} > -0.00223 < U_{coul} > -0.00872 < U_{rxn} > -0.45601 < U_{cav} >$$
$$(n = 11,\ R^2 = 0.998,\ s = 0.243,\ F = 3742.6,\ P \leq 0.001)$$

Because of the robust prediction of free energy of binding, the developed LIE-SGB model was used to determine the $\Delta G_{bind,pred}$ of the newly designed noscapinoids and virtual screening of a panel of highly potent derivatives. Based on the improved $\Delta G_{bind,pred}$ compared to noscapine ($\Delta G_{bind,expt}$ −5.246 kcal/mol), we have selected a panel of three 1,3-diynyl-noscapinoids **20**–**22** (Figure 4) having $\Delta G_{bind,pred,}$ value −6.694, −7.294 and −7.468 kcal/mol, respectively.

All the three 1,3-diynyl noscapinoids **20**–**22** were accommodated very well inside the binding cavity (Figure 5). However, their molecular interactions with the binding site amino acids (within 5 Å) are albeit different as shown in the

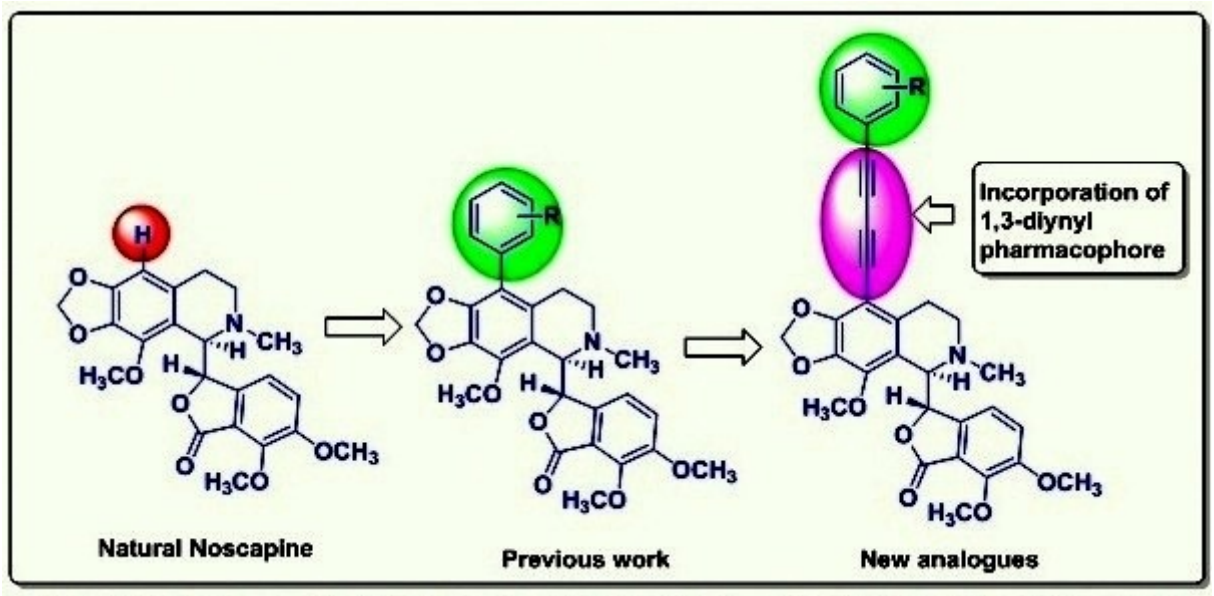

Figure 1. General scheme for strategic development of new noscapine congeners by substitution of various functional groups using in silico combinatorial chemistry.

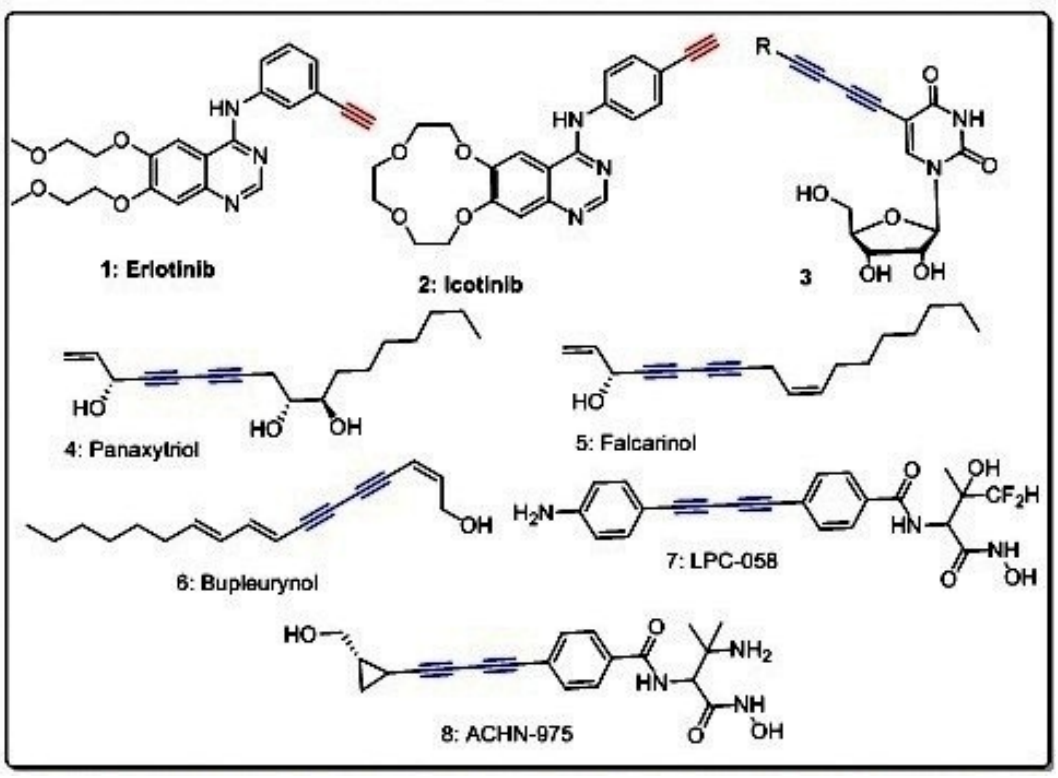

Figure 2. Structures of anticancer drugs **1** and **2** containing ethyne group and 1,3-diyne containing bioactive natural and synthetic products **3**–**8**.

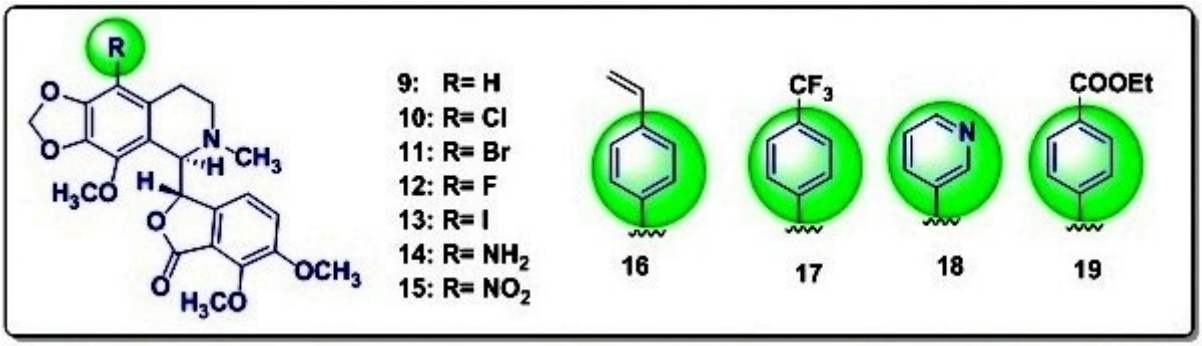

Figure 3. Molecular structures of previously reported noscapine derivatives that have experimentally proven to bind tubulin with known free energy of binding (Table 1) and used as training set molecules for LIE-SGB model building.

ligplot (Figure 6a-c). This might be due to the different functional groups present among themselves. As showed in the figure the most potent 1,3-diynyl noscapinoid **22** in terms of docking score interacts more intensely with the residues of tubulin compared to other two derivatives. Its binding involved 6 hydrogen bonds (dashed lines): the functional group CF_3 form 3 hydrogen bonds with the amine nitrogen (NE_3) of Glu B247 (bond length 3.34 Å), amine nitrogen (N) of Thr A225 (bond length 4.65 Å) and amine nitrogen (N) of Tyr A224 (bond length 3.04 Å); the nitrogen atom of isoquinoline ring of **22** hydrogen bond with side chain group (OG1) of Thr A73 (bond length 3.59 Å); both the oxygen of isobenzofuranone ring of **22** hydrogen bonds with the side chain group (NH_2) of Arg B2 (bond length 4.43 Å) and side chain group (NE) of Arg B2 (bond length 2.92 Å) (Figure 6a). In contrast the 1,3-diynyl noscapinoids **20** and **21** revealed only 3 hydrogen bonds with the binding site residues (Figure 6a,b). Besides, hydrogen bonding, good number of hydrophobic interactions were involved in the binding of 1,3-diynyl noscapinoids **20**–**22** with binding site residues (Supplementary Table S10–S13). Most of the binding site residues are found common in the binding of noscapine and its 1,3-diynyl noscapinoids **20**–**22** such as Gln B247, Glu A77, Glu B47, Arg B48, Pro B245, Ala B250, Gly B246, Glu A71, Thr A73 and Met B1 (Figure 6). The binding site amino acids

Table 1. Molecular docking results (Glide XP) as well as calculated energies using Liasion programme (Schrodinger package) of noscapine and its 1,3-diynyl derivatives: van der Waals energy (U_{vdw}), Columbic energy (U_{coul}), reaction energy (U_{rxn}) and cavity energy (U_{cav}) as well as predicted free energy of binding ($\Delta G_{bind,pred}$) based on LIE-SGB prediction model and experimental free energy of binding ($\Delta G_{bind,expt}$). The newly designed 1,3-diynyl noscapinoids, **20**–**22** revealed improved $\Delta G_{bind,pred}$ compared to the lead molecule, noscapine as well as its previously reported derivatives.

Ligand	Glide XP_{score} (kcal/mol)	$<U_{vdw}>$ (kcal/mol)	$<U_{coul}>$ (kcal/mol)	$<U_{rxn}>$ (kcal/mol)	$<U_{cav}>$ (kcal/mol)	$\Delta G_{bind,\ expt}$ (kcal/mol)	$\Delta G_{bind,pred}$ (kcal/mol)
9	−1.927	−45.14	−330.8	135.5	2.097	−5.246	−5.212
10	−2.038	−49.00	−210.2	116.0	3.283	−6.006	−6.178
11	−2.766	−42.50	−362.1	155.9	4.208	−5.827	−6.060
12	−2.940	−48.06	−355.8	168.7	2.548	−5.587	−5.899
13	−3.263	−47.69	−285.7	135.5	3.103	−6.360	−5.987
14	−4.492	−47.44	−77.3	118.2	3.954	−6.628	−6.668
15	−2.605	−33.39	−331.9	176.7	4.465	−5.551	−5.657
16	−2.287	−45.57	−277.9	112.3	3.285	−5.665	−5.706
17	−2.350	−33.47	−324.5	152.5	3.766	−5.783	−5.151
18	−3.679	−45.41	−471.2	152.8	3.669	−5.673	−5.790
19	−4.687	−42.69	−267.6	129.9	3.465	−5.518	−5.722
20	−3.981	−54.80	−329.0	177.4	2.747	Nd	−6.694
21	−4.770	−53.80	−302.5	123.6	5.147	Nd	−7.294
22	−3.968	−49.87	−301.6	133.9	6.053	Nd	−7.468

$<U_{vdw}>$, $<U_{coul}>$, $<U_{rxn}>$ and $<U_{cav}>$ energy terms represents the ensemble average energy terms calculated as the difference between bound and free state of the ligands and its environment. $\Delta G_{bind,expt}$ was calculated from the dissociation constant (K_d *value*) using the relationship: $\Delta G_{bind,expt} = RT \ln K_d$ where T = 298 K and R = 0.00199 (kcal/mol.K). Nd: not determined.

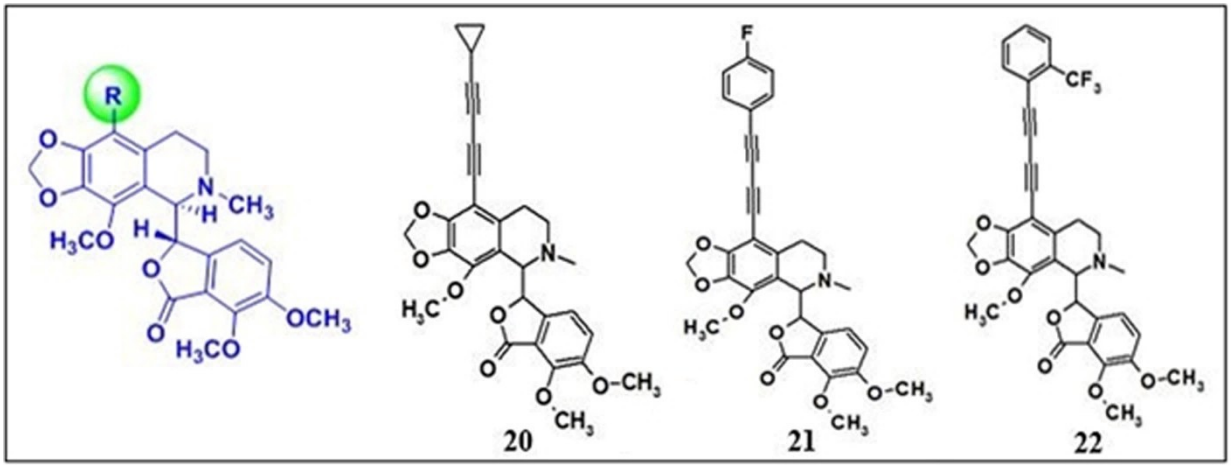

Figure 4. A panel of 1,3-diynyl-noscapinoids developed in the study: 9-cycloro-diyne-noscapine (**20**), 9,4F-ph-diyne-noscapine (**21**) and 9,2-CF_3-ph-diyne-noscapine (**22**).

that are uniquely involved in the binding of 1,3-diynyl noscapinoids **20**–**22** compared to noscapine are Val B355, Pro A72, Arg B2, Lys A96, Arg A221, Met B325, Thr A223, Tyr A224 and Thr A225 (Figure 6). Inspired by our computational findings, we have chemically synthesized the newly designed 1,3-diynyl noscapinoids **20**–**22** to further evaluate their anti-cancer potential.

Predicted ADME properties of noscapine and its 1,3-diynyl derivatives 20–22

In order to validate the lead optimization, we have predicted the absorption, distribution, metabolism, and excretion (ADME) properties of noscapine and its 1,3-diynyl derivatives **20**–**22** using QikProp (Schrodinger software package). A number of ADME properties were predicted viz. molecular weight (*MW*), total solvent accessible surface area (*SASA*), octanol/water partition coefficient (*QPlogPo/w*), octanol/gas partition coefficient (*QPlogPoct*), water/gas partition coefficient (*QPlogPw*), polarizability in cubic angstroms (*QPpolrz*), % human oral absorption in intestine (*QP%*), brain/blood partition coefficient (*QPlogBB*), IC_{50} value for blockage of HERG K+ channel (*QPlogHERG*), skin permeability (*QPlogKp*), prediction of binding to human serum albumin (*QPlogKhsa*), apparent Caco-2 cell permeability in nm/sec (*QPPCaco*) and apparent MDCK cell permeability in nm/sec (*QPPMDCK*). Caco-2 cells are a model for the gut-blood barrier whereas MDCK cells are considered to be a good mimic for the blood-brain barrier. Also we evaluated

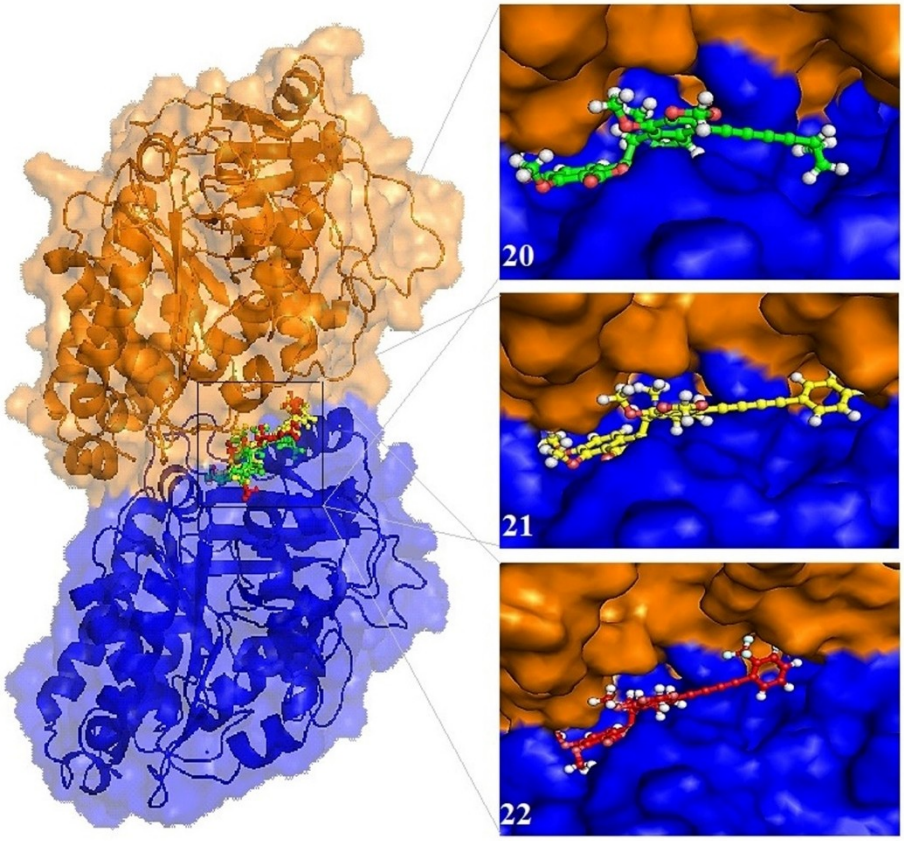

Figure 5. The newly designed 1,3-diynyl noscapinoids **20**–**22** are well accommodated inside the binding pocket at the interface between α- and β-tubulin. The binding of these noscapinoids are biased more towards β-tubulin.

the acceptability of noscapine and its 1,3-diynyl derivatives **20**–**22** based on the Lipinski's rule of 5 (number of violations of Lipinski's rule of five) which is essential for rational drug design. It was interesting to found that noscapine and its 1,3-diynyl derivatives **20**–**22** revealed significant values for the properties analysed and qualified all the drug like characteristic based on Lipinski's rule of 5 (Table 2).

Table 2. A list of properties calculated for Noscapine and its 1,3-diynyl derivatives by Qikprop simulation and used for the ADME screening of the drug molecules. It was found that noscapine and its 1, 3-diynyl derivatives **20**–**22** satisfied all the properties essential for ADME screening.

Sl No.	ADME Screening	Noscapine	**20**	**21**	**22**	Recommended values
1	*MW*	413.4	501.5	555.5	605.6	130–725
2	*SASA*	582.6	815.0	860.0	903.8	300–1000
3	*Accpt HB*	8.75	8.75	8.75	8.75	2.0–20.0
4	*QPpolrz*	37.97	51.90	57.65	60.14	13.0–70.0
5	*QPlogPoct*	17.44	21.18	23.72	24.55	8.0–35
6	*QPlogPw*	10.03	10.49	11.85	11.63	4.0–45.0
7	*QPlogPo/w*	1.61	4.13	5.18	5.87	−2.0–6.5
8	*QPlogHERG*	−4.28	−6.58	−7.58	−7.61	Below −5.0
9	*QPPCaco*	770.5	948.4	967.1	1125.8	<25 poor >500 great
10	*QPlogBB*	0.34	0.17	0.29	0.49	−3.0–1.2
11	*QPPMDCK*	412.9	516.8	954.7	2304.7	<25 poor >500 great
12	*QPlogKp*	−3.96	−3.39	−2.73	−2.76	−8.0–−1.0
13	*QPlogKhsa*	−0.57	0.40	0.69	0.91	−1.5–1.5
14	*QP%*	88.05	91.47	84.83	90.04	>80% high <25% poor
15	*Rule of Five (No. of violations)*	0	1	2	2	Maximum is 4

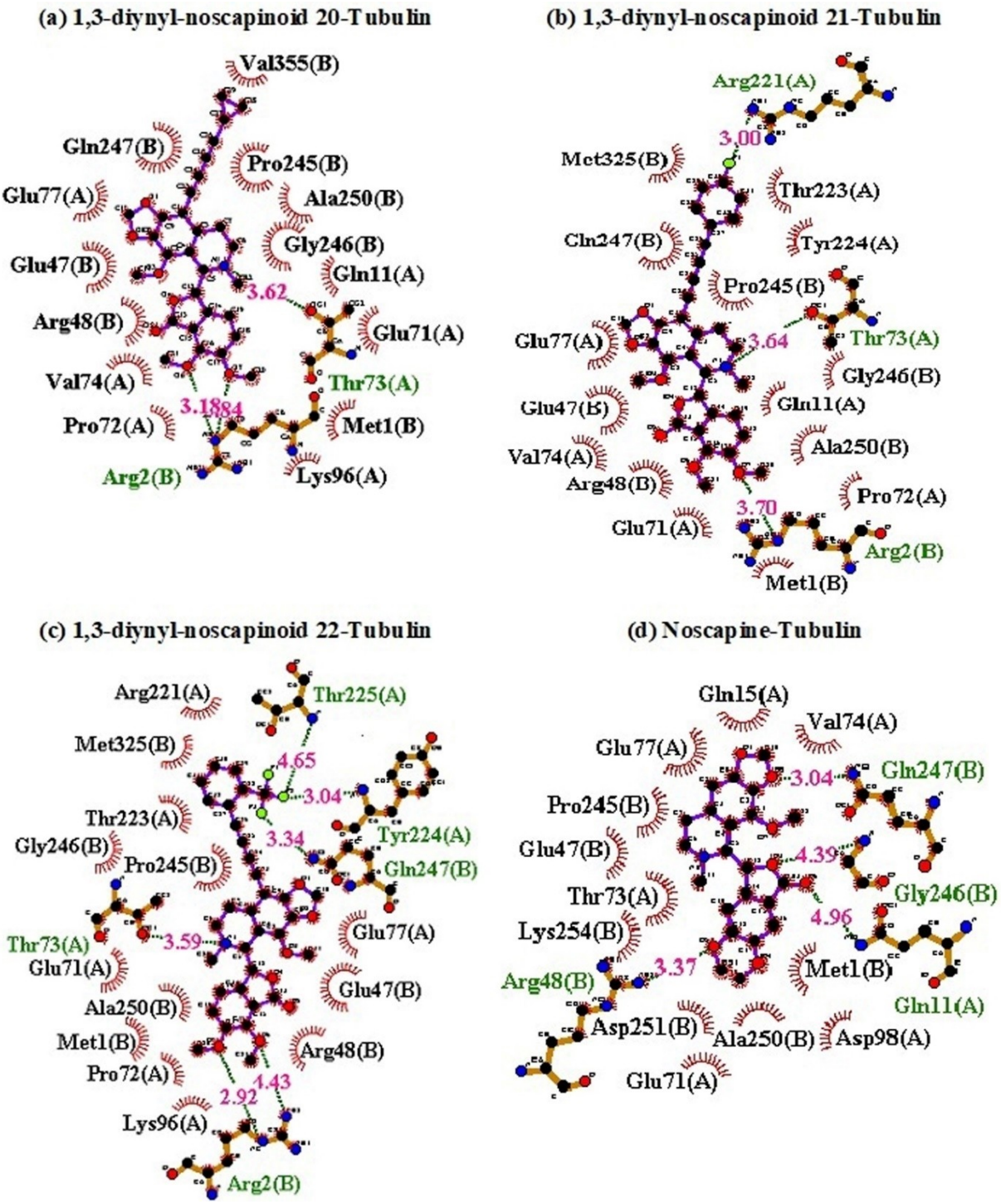

Figure 6. Two dimensional representation of interaction observed between the binding site residues of tubulin with 1,3-diynyl noscapinoids **(a) 20**, **(b) 21**, **(c) 22** and **(d) Noscapine**. Dashed lines denote hydrogen bonds and numbers indicate hydrogen bond lengths in Å. Hydrophobic interactions are shown as arcs with radial spokes. The figure was made using LIGPLOT.[18] The residues within 5 Å distance from the docked ligands were only shown in the figures.

1,3-diynyl noscapinoids inhibits proliferation of cancer cells

Based on our in silico results, we want to determine the anti-proliferative activity of the noscapine and its 1,3-diynyl derivatives **20**–**22** using two human breast adenocarcinoma cells, MCF-7 (estrogen- and progesterone- receptor positive) and MDAMB-231 (estrogen- and progesterone- receptor negative). The compounds were dissolved in DMSO to make a concentration ranging from 5 μM to 100 μM. Sulforhodamine B (SRB) *in vitro* proliferation assay was used to determine the IC_{50}

values (the drug concentration required to achieve a cell kill of 50%). The IC_{50} values for noscapine and its 1,3-diynyl derivatives **20**–**22** for both the cell lines are assembled in Table 3. The rationally designed 1,3-diynyl noscapinoids **20**–**22** exhibited improved cytotoxic activity compared to noscapine using both the cell lines (Figure 7). The IC_{50} value amounted to 35.2, 27.3, 18.7 and 12.7 μM with noscapine, **20**, **21** and **22**, respectively, for MCF-7 cells. Parenthetically, a comparable modest IC_{50} value of 39.6, 31.4, 22.5 and 16.1 μM was measured for noscapine, **20**, **21** and **22**, respectively for MDAMB-231 cells. The anti-proliferative activity of the newly designed derivatives was improved many fold compared to noscapine using both the cell lines. The close IC_{50} values obtained using MCF-7 and MDAMB-231 suggests that these test compounds inhibit cellular proliferation of cancer cells impartial of hormone receptor status. Despite the fact that a significant correlation on the sensitivity of cancer cells to these noscapinoids cannot yet be established at this stage, though it is evident that tubulin represents a potential target for these compounds.

To further support the anticancer efficacy of the 1,3-diynyl noscapinoids **20**–**22** we have performed colony formation assay using a triple negative breast cancer cell line MDAMB-231. The cancer cells were treated with increasing concentration of one of the 1,3-diynyl derivatives of noscapine, **22** and incubated the cells at culture conditions for 10 days for colony formation. The number of colonies formed was determined using image-J software. The inhibition in colony formation was found to be concentration dependent (Figure 8). The number of colonies formation was significantly inhibited by the treated compound compared to untreated cells. The IC_{50} value was found to be 4.0 μM using colonogenic assay.

Besides, the anti-proliferative activity, morphological examination using DAPI staining under the fluorescence microscope revealed apoptotic cell death to MDAMB-231 cancer cells. Alteration in morphological features such as chromatin condensation, plasma membrane blebbing, and appearance of apoptotic bodies with the treatment of 1,3-diynyl noscapinoids **20**–**22** indicated apoptotic cells (Figure 9).

Table 3. IC_{50} values of 1,3-diynyl noscapinoids **20**–**22**. All the rationally designed noscapinoids were found to have improved anti-proliferative activity compared to the lead molecule, noscapine.

IC_{50} (μM)	Noscapine	**20**	**21**	**22**
MCF-7	35.2 ± 2.7	27.3 ± 2.4	18.7 ± 1.9	12.7 ± 1.4
MDA-MB-231	39.6 ± 3.5	31.4 ± 2.8	22.5 ± 2.2	16.1 ± 1.8

1,3-Diynyl derivatives of noscapine alter the cell cycle progression and cause mitotic arrest

In order to determine the mechanism of cellular apoptosis, we examined the effect of noscapine and its 1,3-diynyl derivatives **20**–**22** (25 μM concentration) on the mitotic and apoptotic indices as a function of time in MCF-7 cells, using fluorescence activated cell sorting (FACS). The results are collated in Figure 10. It is revealed that more number of G2/M cells were accumulated at 24 h of treatment with the test compounds and then a decline upto 72 h. In consistent with this, the apoptotic cells also increased in number during this time period (Figure 10). Microtubule-interfering agents, including noscapine,[3,8] are well known to arrest cell cycle progression at the G2/M phase in mammalian cells.[19] The cell cycle profile of MCF-7 with treatments of noscapine and its 1,3-diynyl derivatives based on FACS analysis is covered in Figure 11 (panels A–E). It has been seen that accumulation of fluorescently labeled DNA is a good indicator to observe the cell cycle progression and cell death.[3,8,12] Cells with 2 N DNA represent the G1 phase,

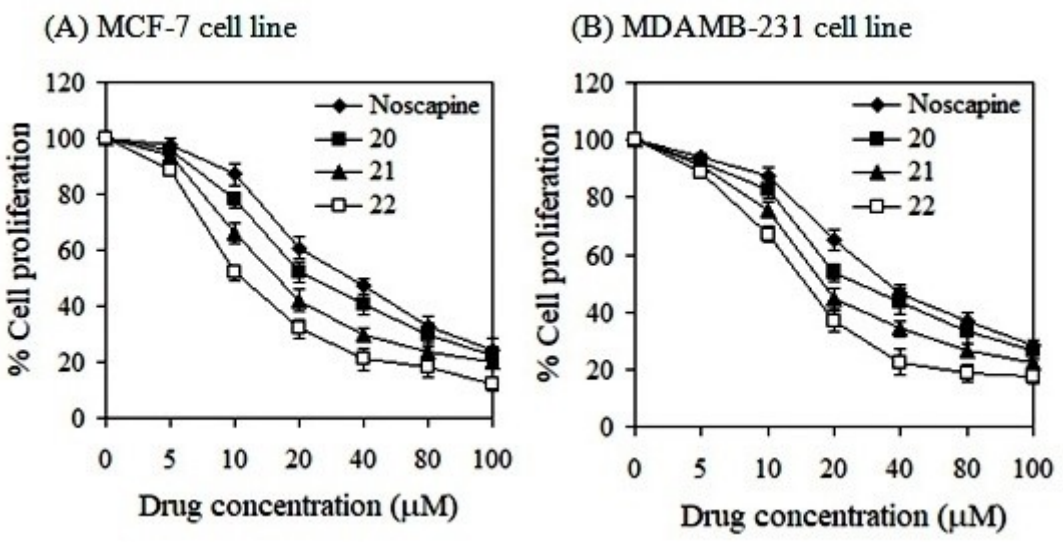

Figure 7. The 1,3-diynyl noscapinoids **20**–**22** are more active compared to noscapine in inhibiting the proliferation of human breast cancer cells. Both (A) MCF-7 and (B) MDAMB-231cells were treated with noscapine and its 1,3-diynyl derivatives, **20**–**22** for 72 h and IC_{50} values were then measured. Each value represents the average of 3 independent experiments.

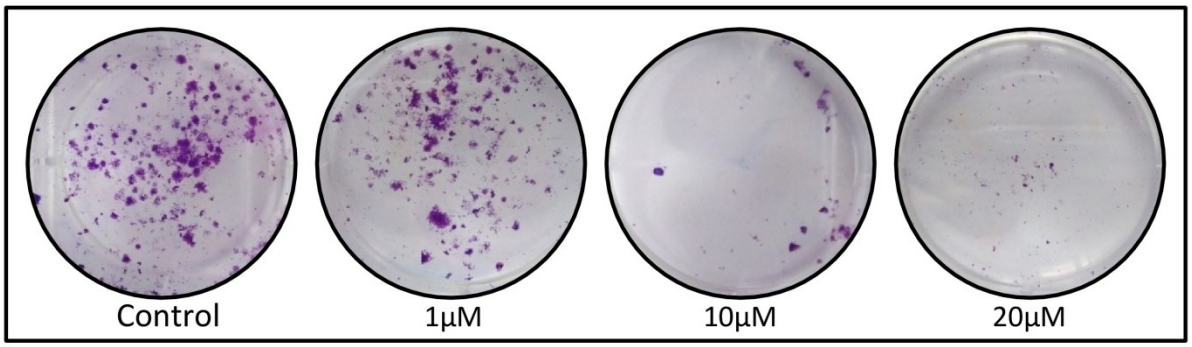

Figure 8. Inhibition in colony formation with the treatment of 1,3-diynyl derivative of noscapine, **22**. The triple negative cancer cell line MDAMB-231 was treated with increasing concentration (1 μM, 10 μM and 20 μM) of the compound. The number of colony formation was significantly inhibited by the compound compared to untreated cells.

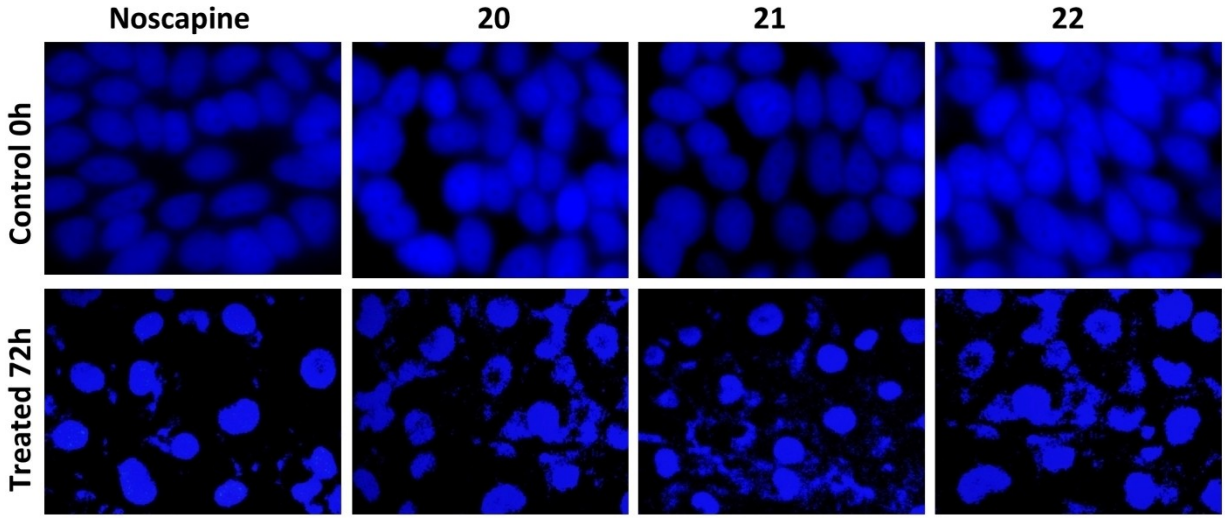

Figure 9. Morphological characterization of MDAMB-231 cancer cells with DAPI staining. Panels show morphological evaluation of nuclei stained with DAPI from control cells (upper panels) and cells treated with IC_{50} concentration (39.6, 31.4, 22.5 and 16.1 μM) of noscapine and its 1,3-diynyl derivatives **20**–**22** (lower panels) for 72 hours using fluorescence microscopy.

while cells with duplicated 4 N DNA represent G2 and M phases. Cells in the process of DNA replication have peaks between 2 N and 4 N, which represent S phase. Cells with less than 2 N DNA represent dying cells that degrade their DNA to different extents. MCF-7 cells treated with 25 μM of the test compounds for 72 h led to significant perturbations of the cell cycle profile. FACS analysis revealed high accumulation of cells in the G2/M phase at 72 h of treatment of noscapine and its 1,3-diynyl derivatives compared to untreated cells. In contrast to G2/M block, a characteristic peak with hypodiploid DNA content (sub-G1) was seen to appear at 72 hours of treatment.

Induction of apoptosis

We next approached to work out whether or not interference with the cell cycle progression by noscapine and its 1,3-diynyl derivatives led to apoptosis cell death. Biochemically the apoptotic cell death is characterized by alterations of lipid composition of cell membrane, in which the phosphatidylserine (PS), normally located on the inner leaflet of the cell membrane, translocates to the outer leaflet, which can be measured by annexin V binding. Further, a cell-impermeant DNA-binding fluorescent dye, propodium iodide can only enter the cells when it is at the stage of late apoptosis when membrane permeability is compromised. The apoptotic cells can be quantified in large extent by FACS analysis. The percentage of early apoptotic and late apoptotic MCF-7 cells for the treatment of noscapine and its 1,3-diynyl derivatives **20**–**22** with a concentration of 25 μM for 72 h is collated in Figure 12 (panels B–E). After 72 h of culture, the control untreated cell culture contained only very few early apoptotic (2.2%) and late apoptotic cells (4.8%), which were considered as the background cell death due to regular trauma during cell culture (Figure 12A). In contrast, the percentage of early apoptotic cells to 5.4%, 13.8%, 16.6% and 24.9% as well as late apoptotic cells to 18.5%, 37.4%, 41.5% and 46.8% with

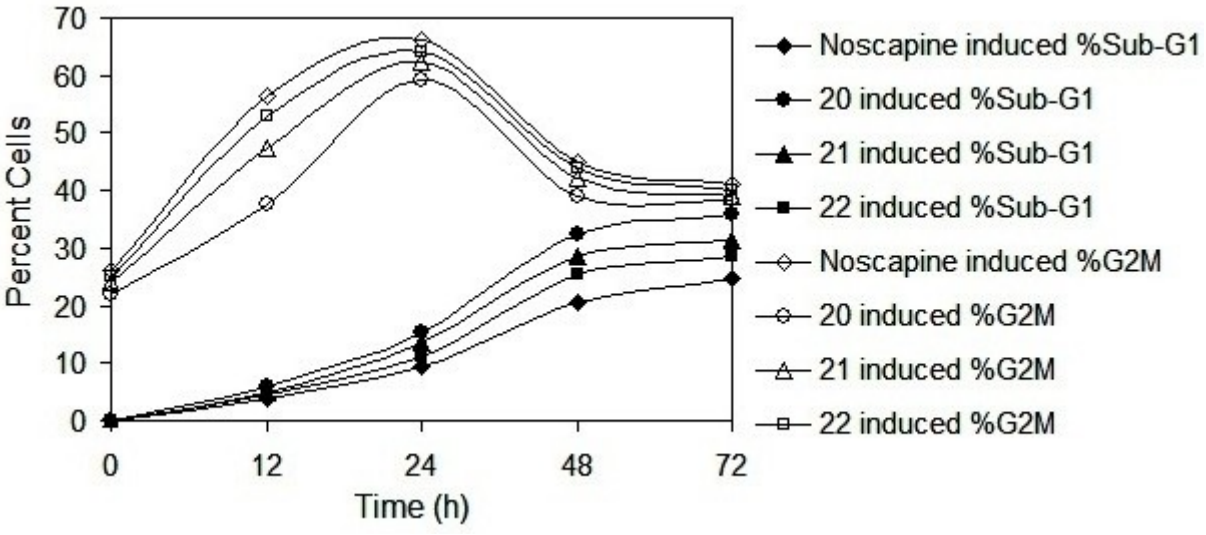

Figure 10. Apoptotic and mitotic index as a function of time of treatment with 25 μM concentrations of noscapine and its 1,3-diynyl derivatives in human breast carcinoma cells (MCF-7). At 24 h, the percentage of G2 M (mitotic cells) cells were 66.2%, 59.3%, 62.4% and 64.2% respectively for noscapine, **20**, **21** and **22**. The increase activity of 1,3-diynyl derivatives compared to noscapine in induction of apoptosis was also evident by the higher percentage of cells with degraded DNA, in that, 24.9%, 35.8%, 31.2% and 28.4% of cells with <2 N DNA (sub-G1) content were seen on treatment of noscapine, **20**, **21** and **22**, respectively.

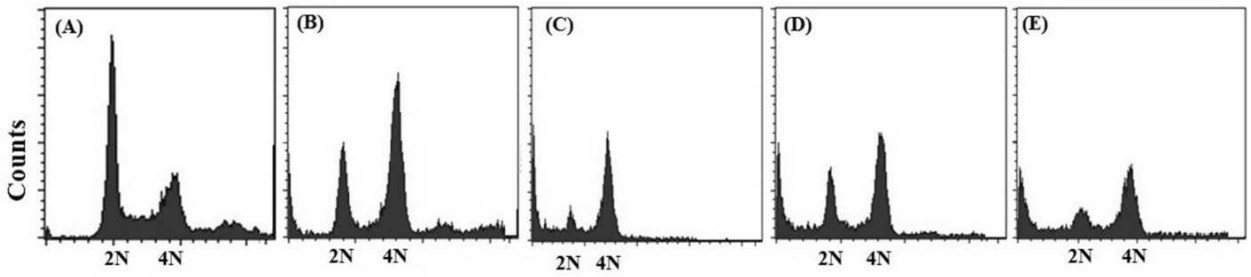

Figure 11. Noscapine and its 1,3-diynyl derivatives, **20**–**22** alter the cell cycle profile, followed by the appearance of a characteristic peak of hypodiploid (sub-G1) DNA content, which indicate induction of apoptosis. Panels A–E depicted analyses of cell cycle progression as determined by FACS in MCF-7 cells treated with 25 μM of noscapine and its derivatives **20**–**22** at 72 hours.

noscapine, **20**, **21** and **22**, respectively was found to be significantly high compared to controlled untreated cells (Figure 12).

In an effort to characterize induced necrobiosis by noscapine and its 1,3-diynyl derivatives **20**–**22**, we performed the TUNEL assay on formalin-fixed MCF-7 cells. The terminal stage of apoptosis display cleaved 3′ ends of DNA which is visualized by specific labeling by TUNEL assay. The quantitative FACS analysis revealed 57%, 59.2%, 62.5% and 68.4% TUNEL-positive cells on treatment with 25 μM noscapine, **20**, **21** and **22**, respectively (Figure 13B–E). In contrast, control untreated cells showed only 3.7% TUNEL-positive cells (Figure 13A).

1,3- diynyl derivatives of noscapine quenched the intrinsic fluorescence of tubulin

Microtubules are autofluorescent by nature due to presence of aromatic amino acids, tryptophan which can be selectively measured by exciting at 295 nm. Any chemical compounds that bind with tubulin and alter its conformation lead to decrease in its intrinsic fluorescence.[3] This is a standard assay to test whether a chemical compound binds to tubulin or not.[8] We have used similar assay to test whether the 1,3-diynyl derivatives of noscapine also bind to tubulin or not. It was revealed that intrinsic fluorescence of tubulin, decreased in presence of 1,3-diynyl derivatives of noscapine **20**–**22**, suggests the binding capability of these compounds to tubulin. The relative percentage of decrease in fluorescence intensity was 12.91%, 18.87% and 27.15% respectively in presence of 25 μM concentration of **20**–**22** (Figure 14), compared to control.

1,3-diynyl derivatives of noscapine alter the secondary structure of tubulin

Circular dichroism is an insightful method of elucidating changes in the secondary structure of the proteins. This can

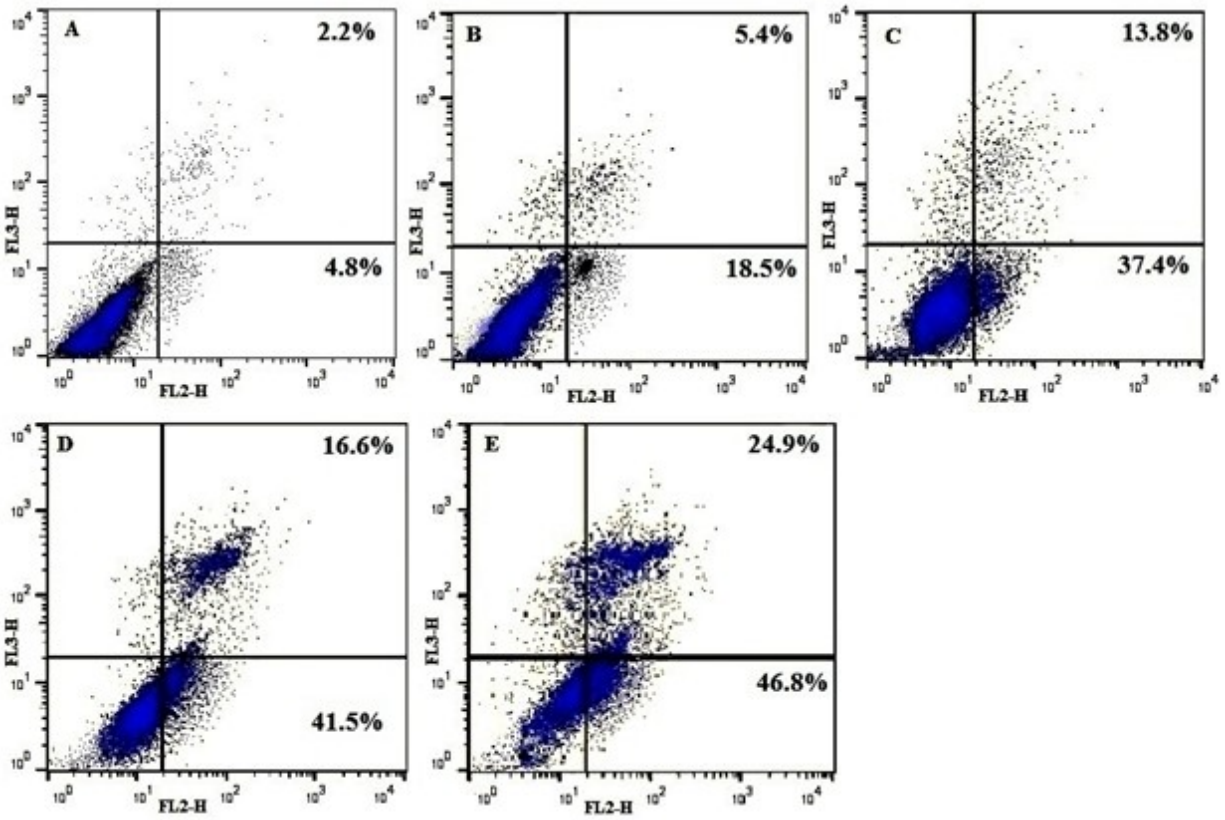

Figure 12. Flow cytometry analysis of phosphatidylserine (PS) exposure in MCF-7 cells treated with noscapine (B) and its derivatives, **20** (C), **21** (D) and **22** (E) with 25 μM for 72 hours and compared with non treated control cells (A). Annexin-V and propidium iodide (PI) were used to distinguish among three sub-populations of cells: PI- and AnnexinV- cells represent viable cells with intact membrane and preserved amino-phospholipid asymmetry, PI- and Annexin V+ cells represent early apoptotic cells with intact cellular membrane exposing phosphatidylserine, whereas PI+ and Annexin V+ cells represent late apoptotic cells with compromised asymmetry and membrane permeability. Representative results of three independent experiments.

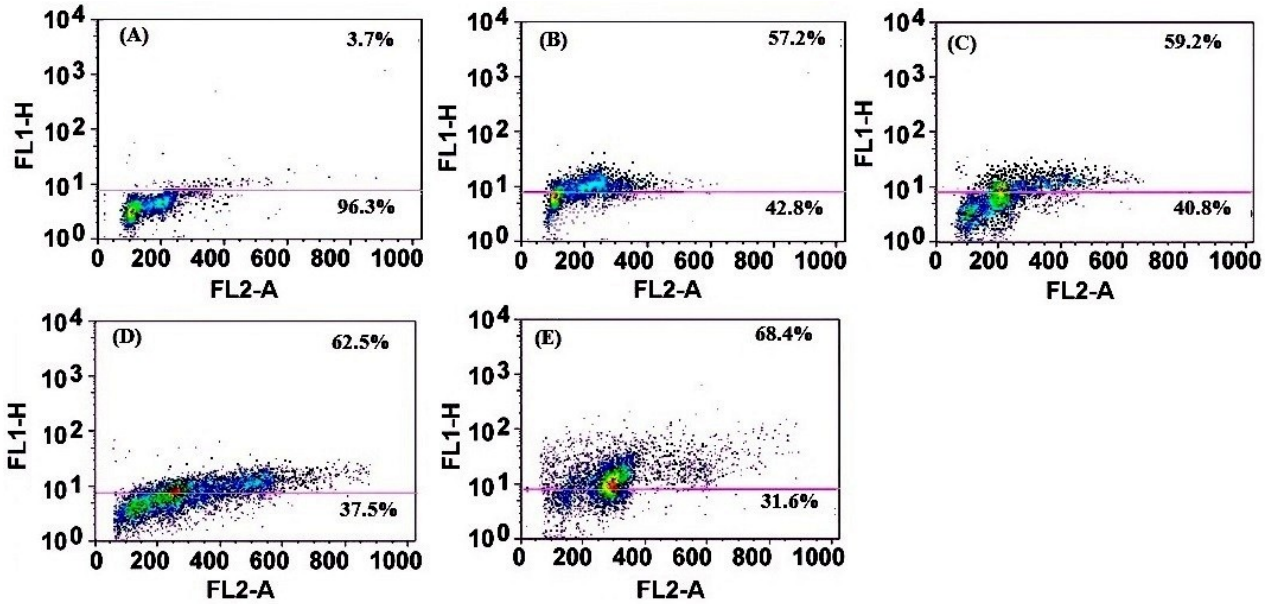

Figure 13. TUNEL analysis reveals induction of apoptosis by (A) untreated cells, (B) noscapine treated cells and its 1,3-diynyl derivatives treated cells: (C) **20**, (D) **21** and (E) **22**, as evidenced by DNA fragmentation in MCF-7 cells. Number of apoptotic cells is indicated by the number of Alexa Fluor 488 positive cells of the total gated cells. The values presented on cytogram is the percentage of apoptotic cells (top) and normal cells (bottom).

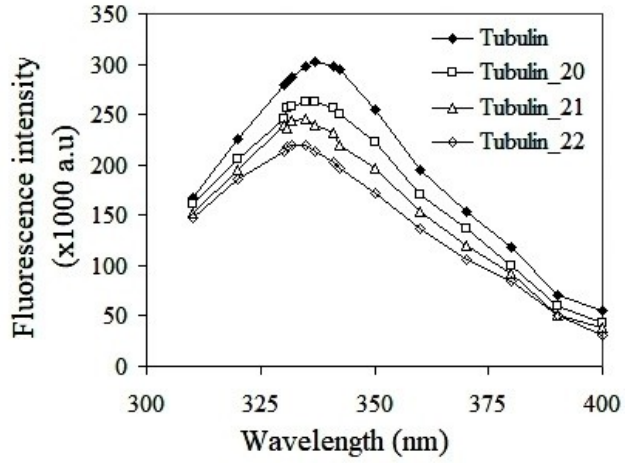

Figure 14. Treatment of purified tubulin with 1,3-diynyl derivatives of noscapine **20**–**22** at a concentration of 25 μM quenched the intrinsic fluorescence of tubulin significantly compared to untreated tubulin. The relative percentage of decreased in fluorescence intensity was 12.91%, 18.87% and 27.15% respectively in presence of 25 μM concentration of **20**–**22** compared to control. Emission spectra were collected in a range of 310 nm–400 nm.

also be used to study the interaction of ligands with protein. The interaction with ligands can influence by various intermolecular as well as intramolecular forces, affecting the protein's secondary and tertiary structure.[20] The elliptical shifts with the treatment of 1,3-diynyl derivatives of noscapine **20**–**22** at a 25 μM concentration revealed a marked disturbance in the structure of the alpha helix (Figure 15), indicating that these molecules interact with the secondary structure of the tubulin.

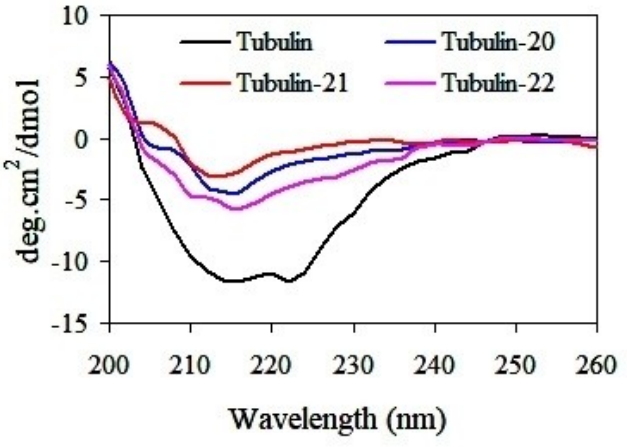

Figure 15. Far-UV circular dichroism spectra indicating disruption of tubulin secondary structure with the treatment of 25 μM concentration of 1,3-diynyl derivatives of noscapine **20**–**22**. The graph represents one of the three independent experiments.

Conclusion

In conclusion, we have strategically designed a panel of 1,3-diynyl derivatives of natural lead molecule, noscapine, in quest of accelerating its anticancer activity. We have also provided the simplest methods for the direct and regioselective modification of noscapine scaffold to produce the 1,3-diynyl derivatives in high yields. All the 1,3-diynyl derivatives developed have showed increase anti-proliferative activity to cancer cells based on our extensive molecular modeling and cellular study using two human breast cancer cell lines, MCF-7 and MDAMB-231. Therefore, these novel compounds may prove efficacious not only in the treatment of breast carcinoma, but also for other type of cancers. Our results compel us to continue to examine the effects of these novel compounds on in vivo animal experiment with the final goal of taking it to the human clinical study.

Supporting Information Summary

For the experimental section, structural characterization of the compounds based on ^{1}H-NMR, ^{13}C-NMR, HRMS Spectra as well as the details regarding the hydrogen bonding and hydrophobic interactions of the ligands with the binding site residues, refer to the supporting information.

Acknowledgements

This work was supported by the Science and Technology Department, Govt. of Odisha [Grant Number: ST-(Bio)-02/2017]. CSIR-IICT communication No. IICT/Pubs./2021/084.

Conflict of Interest

The authors declare no conflict of interest.

Keywords: 1,3-diynyl-noscapinoids · Anticancer activity · Antitumor agents · Breast cancer · Drug Discovery · Drug Design · Noscapine · Tubulin binding

[1] J. J. Kavanagh, A. P. Kudelka, *Curr. Opin. Oncol.* **1993**, *5*, 891–899.
[2] E. K. Rowinsky, R. C. Donehower, *Pharmatherapeutica* **1991**, *52*, 35–84.
[3] K. Ye, Y. Ke, N. Keshava, J. Shanks, J. A. Kapp, R. R. Tekmal, J. Petros, H. C. Joshi, *Proc. Natl. Acad. Sci. USA* **1998**, *95*, 1601–1606.
[4] B. Dahlstrom, T. Mellstrand, C. G. Lofdahl, M. Johansson, *Eur. J. Clin. Pharmacol.* **1982**, *22*, 535–539.
[5] M. O. Karlsson, B. Dahlstrom, S. A. Eckernas, M. Johansson, A. T. Alm, *Eur. J. Clin. Pharmacol.* **1990**, *39*, 275–279.
[6] L. N. Jensen, L. L. Christrup, L. Jacobsen, J. Bonde, H. Bundgaard, *Acta Pharm. Nord.* **1992**, *4*, 309–312.
[7] J. W. Landen, R. Lang, S. J. McMahon, N. M. Rusan, A. M. Yvon, A. W. Adams, M. D. Sorcinelli, R. Campbell, P. Bonaccorsi, J. C. Ansel, D. R. Archer, P. Wadsworth, C. A. Armstrong, H. C. Joshi, *Cancer Res.* **2002**, *62*, 4109–4114.
[8] J. Zhou, K. Gupta, J. Yao, K. Ye, D. Panda, P. Giannakakou, H. C. Joshi, *J. Biochem.* **2002** (b), *277*, 39777–39785.
[9] J. Zhou, K. Gupta, S. Aggarwal, R. Aneja, R. Chandra, D. Panda, H. C. Joshi, *Mol. Pharm.* **2003**, *63*, 799–807.

[10] J. W. Landen, V. Hau, M. Wang, T. Davis, B. Ciliax, B. H. Wainer, E. G. Van Meir, J. D. Glass, H. C. Joshi, D. R. Archer, *Clin. Cancer Res.* **2004**, *10*, 5187–5201.
[11] P. K. Naik, M. Lopus, R. Aneja, S. N. Vangapandu, H. C. Joshi, *J. Comp. Aid. Mol. Des.* **2012**, *26*, 233–247.
[12] R. Aneja, S. N. Vangapandu, M. Lopus, R. Chandra, D. Panda, H. C. Joshi, *Mol. Pharm.* **2006** a, *69*, 1801–1809.
[13] R. Aneja, S. N. Vangapandu, M. Lopus, V. G. Viswesarappa, N. Dhiman, A. Verma, R. Chandra, D. Panda, H. C. Joshi, *Biochem. Pharmacol.* **2006** b, *72*, 415–426.
[14] S. Santoshi, N. K. Manchukonda, C. Suri, M. Sharma, B. Sridhar, S. Joseph, M. Lopus, S. Kantevari, I. Baitharu, P. K. Naik, *J. Comp. Aid. Mol. Des.* **2015**, *29*, 249–270.
[15] N. Jain, D. Yada, T. B. Shaik, G. Vasantha, P. S. Reddy, S. V. Kalivendi, B. Sreedhar, *ChemMedChem* **2011**, *6*, 859–868.
[16] X. Liang, R. Gopalaswamy, I. I. I. F. Navas, E. J. Toone, P. Zhou, *J. Org. Chem.* **2016**, *81*, 4393–4398.
[17] C. J. Lee, X. Liang, Q. Wu, J. Najeeb, J. Zhao, R. Gopalaswamy, P. Zhou, *Nat. Commun.* **2016**, *7*, 1–7.
[18] A. C. Wallace, R. A. Laskowski, J. M. Thornton, *Protein Eng. Des. Sel.* **1995**, *8*, 127–134.
[19] M. A. Jordan, L. Wilson, *Met. Cell. Bio.* **1998**, *61*, 267–291.
[20] S. M. Kelly, T. J. Jess, N. C. Price, *Biochim. Biophys. Acta.* **2005**, *1751*, 119–139.

Submitted: December 18, 2020
Accepted: March 31, 2021